

Article

Quantifying Dry and Wet Deposition Fluxes in Two Regions of Contrasting African Influence: The NE Iberian Peninsula and the Canary Islands

Sonia Castillo ¹, Andrés Alastuey ¹, Emilio Cuevas ², Xavier Querol ¹ and Anna Avila ^{3,*}

¹ Institute of Environmental Assessment and Water Research (IDAEA, CSIC), C/Jordi Girona 18–26, 08034 Barcelona, Spain; sonia.castle@gmail.com (S.C.); andres.alastuey@idaea.csic.es (A.A.); xavier.querol@idaea.csic.es (X.Q.)

² Izaña Atmospheric Research Centre (AEMET), C/La Marina 20, 38001 Santa Cruz de Tenerife, Spain; ecuevasa@aemet.es

³ Center for Ecological Research and Forestry Applications (CREAF), Universitat Autònoma de Barcelona, 08193 Bellaterra, Spain

* Correspondence: anna.avila@uab.cat; Tel.: +34-9-3581-4669

Academic Editors: George Kallos and Marina Astitha

Received: 28 February 2017; Accepted: 15 May 2017; Published: 18 May 2017

Abstract: This study considers the role of distance to the African source on the amount of deposition. To this end, dry and wet deposition was measured at a site close to Africa (Santa Cruz de Tenerife in the Canary Islands, SCO) and at a distant site located in NE Spain (La Castanya, Montseny, MSY). Because of the important influence of African influence on the buildup of particles in the atmosphere, we specifically addressed the contribution of North African events (NAF events) compared to other provenances (no-NAF events) in the wet and dry pathways at the two sites. At the site close to Africa, most of the crustal-derived elements were deposited in the dry mode, with NAF events contributing more than no-NAF events. Marine elements, by contrast, were mostly deposited at this site in the wet form with a predominance of no-NAF events. At MSY, wet deposition of SO₄-S, NO₃-N and NH₄-N during NAF events was higher than at the site close to Africa, either in the wet or dry mode. This fact suggests that mineral dust interacts with pollutants, the mineral surface being coated with ammonium, sulphate and nitrate ions as the dust plume encounters polluted air masses in its way from North Africa to the Western Mediterranean. African dust may provide a mechanism of pollution scavenging and our results indicate that this removal is more effective in the wet mode at sites far away from the mineral source.

Keywords: mineral dust; dry deposition; wet deposition; African intrusions; particulate matter; anthropogenic pollution

1. Introduction

Deposition fluxes from the atmosphere contribute significantly to ecosystems by providing elements of biogeochemical relevance, such as N, Ca, Mg, K, P and Fe [1,2]. Atmospheric deposition can occur through wet or dry pathways. Wet deposition (WD) is the process by which gases and aerosols are deposited on the earth's surface mainly in the form of rain, snow or mist [3] and is usually measured with collectors specifically designed to exclude dry deposition and expose the collecting surface only during periods of precipitation. Dry deposition (DD) of gases and particles occurs by diffusion, turbulent and Brownian transfer and by gravitational settling from the atmosphere to the surfaces [4,5]. DD can involve large particles, small particles and gases, alone or combined. Many different methods have been proposed to measure DD, as deposition processes differ depending on the physical and chemical form of the considered elements and the characteristics of the receptor

surfaces [4–6]. In arid and semi-arid regions subject to high dust deposition, the collection of the dryfall flux in buckets or funnels has been considered adequate because of the predominantly coarse nature of the particles which tend to settle by gravity [7–12]. Consequently, this is the method that we will use in this work.

The amount and characteristics of atmospheric deposition will depend on the local atmospheric pollutant load, the meteorology and the transport patterns from emission sources to receptor sites. The Iberian Peninsula, located between Europe and Africa and surrounded by the Mediterranean Sea and Atlantic Ocean, is largely affected by marine aerosols, urban/industrial pollutants from European and North African sources and mineral dust from North African arid areas [13–15]. The Canary Islands, located in the Atlantic Ocean at a distance of 350 km from the North African coast, are highly impacted by marine aerosols and African dust, though aerosols of local urban/industrial origin also have a role [16–18].

Previous studies in the Mediterranean have shown a latitudinal gradient of atmospheric coarse aerosol levels linked to the African influence, with an increasing contribution from northern to southern latitudes [15,19]. This suggests the role of distance in shaping the concentration levels and deposition amounts in this region and motivates the present study of comparing the deposition fluxes at two sites located at different distances from the African continent: Santa Cruz de Tenerife in the Canary Islands (SCO) and Montseny (MSY) in the Northeast of the Iberian Peninsula.

Several studies have provided estimates on the relative role of DD vs. WD in the Mediterranean region [8,9] and in some specific locations from the Iberian Peninsula [10,12,20–23], but only a few of these have provided data on wet and dry fluxes by also taking into account the role of the African contribution. In the Canary Islands, information on WD and DD is very scarce. To knowledge, only [24] reported on WD and DD fluxes, but their study only considered deposition of particulate matter.

For coarse particles (PM₁₀), the gravitational dust settlement may constitute the main deposition flux for sites with low precipitation [12,25,26]. Thus, it is expected that DD will overcome WD for elements associated with coarse particles at the site in the Canary Islands, whilst this predominance will be lost as distance from Africa increases, implying that WD may be the predominant deposition flux at the Montseny site. As far as the authors know, this type of study has not yet been tackled, and the current study addresses this knowledge gap by considering the effect of distance to the African source and the particular meteorology of the sites on the amount and type of deposition. Specifically, at both sites, we quantify the WD and DD fluxes of major soluble elements and determine the contribution of the African dust source to these deposition fluxes.

2. Study Area and Meteorological Conditions

The sampling areas were selected in locations with different meteorological conditions and different distances from the Sahara desert (Figure 1).

The SCO site is located in the Canary Islands, in Santa Cruz de Tenerife (Figure 1) at the facilities of the Air Quality Research Observatory at Santa Cruz de Tenerife (28°28' N, 16°14' W; 52 m.a.s.l.) that belongs to the Izaña Atmospheric Research Center, from the State Meteorological Agency of Spain (AEMET). Santa Cruz de Tenerife has an annual mean precipitation around 225 mm and an annual mean temperature of 21.5 °C (<http://www.aemet.es/>).

The site in the Montseny Mountains (MSY, 41°46' N, 2°21' E; 700 m.a.s.l.) is located 40 km NNE from Barcelona and 25 km from the Mediterranean coast (Figure 1). The climate in Montseny is meso-Mediterranean sub-humid, with high interannual variability in precipitation (in the period 1980–2009 annual precipitation at the MSY site varied from 503 to 1638 mm, the arithmetic mean being of 840 mm). Summer droughts are common, though often attenuated by frequent orographic storms. Mean air temperature at MSY was 9.2 °C during the period 1980–2000. During the study period, the highest mean temperatures and lowest precipitation rates were recorded during the heat wave year of 2003. Conversely, 2002 was characterized by a summer with anomalously low temperatures and high precipitation.

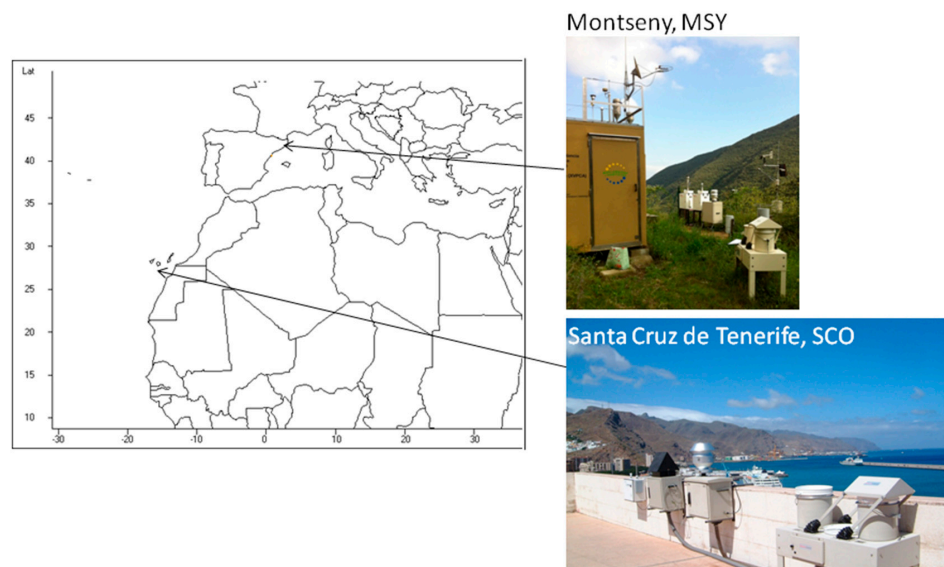


Figure 1. Map of the study sites in Montseny (MSY) and Santa Cruz de Tenerife (Canary Islands, SCO) and photos of the instrumentation at the sites. In the forefront of both photos, the wet/dry deposition collector is shown.

Atmospheric Dynamics of the Sites

The atmospheric circulation over North-western Africa is determined by the trade winds that flow from the northeast and the Saharan Air Layer (SAL), which conveys uplifted dust from the Sahara in a westward direction to the subtropical North Atlantic [27–29]. In summer, high temperatures cause large-scale convection movements that set the SAL at altitudes up to 6 km above the boundary layer [29,30], while in winter and spring, the SAL is located at 2–3 km, intruding into the marine boundary layer [31]. The Canary Islands have quite stable meteorological patterns determined by the position of the Azores high and the quasi-permanent action of the trade winds that flow from the NE [32,33], resulting in a strongly stratified low troposphere. A quasi-permanent and stable temperature inversion limited at altitudes around 700–1300 m.a.s.l. in summertime and between 1400 and 1800 m.a.s.l. in wintertime is observed [33]. This temperature inversion separates a dry, free troposphere from a relatively fresh and humid oceanic boundary layer [31–33]. The dominance of the trade winds in the marine boundary layer plays a key role in the atmospheric dynamics of the Islands, favouring the dispersion of pollutants from urban and industrial sites over the ocean.

Despite this general pattern towards the west, large quantities of dust are also carried to the Mediterranean and south Europe [15,34,35]. In the western Mediterranean, the atmospheric circulation is highly influenced by the Azores High [36]. In winter, the location of the Azores High favours the entry of Atlantic air masses into the Mediterranean basin that contributes to reduce the levels of atmospheric pollutants by replacing the existing air masses [13,37]. In summer, the synoptic scenario favours weak pressure gradients in the Mediterranean basin, and consequently, local circulations dominate the dynamics of the area, enhancing the accumulation of pollutants [38,39]. The low rainfall and the high photochemical activity in summer further contribute to increase the levels of particles in the area [39]. In winter, the MSY station is usually above the mixing layer and is less affected by the regional anthropogenic pollution. In summer, the station is included in the expanded mixed layer, and thus it is affected by the regional pollution [36,40]. In the Mediterranean, Saharan dust outbreaks occur on 20–40% of the days in a year, and the African contribution to the particulate load is inversely related to latitude [15]. Dust intrusions to south Europe mostly occur in summer when a persistent surface thermal low is formed over North Africa so that the North African high moves to upper atmospheric levels [17,41]. High pressures under these conditions prevent the formation of clouds, favoring deposition in the dry mode. By contrast, when depressions are formed over the west of the

Iberian Peninsula or in the western Mediterranean basin, the uplifted African dust is incorporated in frontal systems that cross the Iberian Peninsula and the southern Mediterranean Sea in an eastward direction. These dust-laden rainfall episodes, which mainly occur in late winter spring and autumn, produce pulses of high African dust deposition in the wet mode [12,14,42].

3. Material and Methods

3.1. Sampling

Data reported here correspond to the hydrologic year defined from 1 August 2002 to 31 July 2003. In this period, the sites were visited weekly and dry and wet samples (in case that rain had occurred during the period) were collected from the dry/wet deposition collector. For DD, most sampling periods were biweekly at SCO, while at MSY only on a few occasions was the DD sampling biweekly. Biweekly sampling ensured high concentrations of the elements for analysis from the DD samples. WD was collected weekly, transporting a subsample of the accumulated rainfall during the week to the laboratory for analysis. At SCO, no DD samples were available for June and July 2003 due to apparatus failure, but no WD data were lost because there was no rain during these months. Missing DD in June and July 2003 was estimated considering that the average weekly deposition DD value from the rest of the year was representative of the missing period. The deposition for the missing months at SCO was calculated and added to complete the year.

The dry/wet deposition collector (G78-1001 ESM Andersen model, ThermoAndersen, Smyrna, GA, USA) is provided with two buckets 40 cm high with a diameter of 29.1 cm, placed on a table at 80 cm height to prevent including local coarse particles from the ground. A movable lid covers the wet deposition bucket during dry periods and is moved to cover the dry one at the onset of rain events. Twenty minutes after the end of the rain, the lid shifts to cover the dry bucket. DD samples were recovered by rinsing the bucket with 250 mL of MilliQ grade distilled water. WD samples consisted of 250 mL of the weekly accumulated precipitation in the wet bucket. After each sampling, buckets were cleaned in situ with abundant MilliQ-grade distilled water. Blanks of MilliQ water were analyzed with the samples to check for the quality of sampling. The volume of the wet bucket was measured prior to sampling and the amount of precipitation was obtained considering the area of the bucket. Also, precipitation at 15-min intervals was recorded with a tipping bucket rain gauge connected to a data logger.

3.2. Chemical Analysis

Upon sampling, pH, conductivity and alkalinity were measured in unfiltered samples over a lapse period of maximum 48 h. pH was measured with a Orion pH-meter equipped with a specific probe for rain samples. Alkalinity was determined by a conductometric method [43] for samples of pH > 5.6. The alkalinity for the scarce number of samples of pH < 5.6 was deduced from pH assuming that the principal component of alkalinity at these sites is bicarbonate, and applying the equilibrium equations of the carbonate system. When discussing results of deposition fluxes, alkalinity has been recalculated as HCO_3^- -C considering that bicarbonate is the dominant component of alkalinity, which is an acceptable approximation for the studied sites (Avila 1996).

Collected water (either WD or DD) was filtered through 0.45 μm cellulose nitrate Millipore filters (HAWPO4700, 47 mm of diameter, MerckMillipore, Billerica, MA, USA).

An aliquot of each filtered sample was acidified with 1% HNO_3 for the analysis of major elements by ICP-OES (Inductively Coupled Plasma Optical Emission Spectrometry, IRIS Advantage TJA solutions, THERMO, Waltham, MA, USA). An unaltered aliquot was used for the analysis of soluble anions (SO_4^{2-} , NO_3^- and Cl^-) and ammonium (NH_4^+) by Ion Chromatography (Dionex 100). For the analyzed elements, average precision and accuracy were lower than the typical analytical errors for ICP-OES (3–5%). The quality of data was further verified by the ionic balance method. The ionic balance in a solution is represented by the cation/anion ratio ($\Sigma\text{cat}/\Sigma\text{an}$) as an indicator for the completeness of the measured ions, which should approach 1 (number of cations is equal to number of anions). The deviation from the

unit indicates that some of the ions are excluded and/or the analytical uncertainty. An allowance of 20% around the central value was admitted (0.8–1.2). In our analysis, the sum of the cations (Na^+ , K^+ , Ca^{2+} , Mg^{2+} and NH_4^+) against the sum of anions (Alkalinity, NO_3^- , SO_4^{2-} and Cl^-), both in WD and DD, showed good $\Sigma\text{cat}/\Sigma\text{an}$ ratios with averages (\pm std. dev) of 1.15 (± 0.35) and 1.08 (± 0.21) in wet and DD, respectively, at MSY, and 1.01 (± 0.16) and 1.14 (± 0.22), respectively, at SCO.

Some elements (X) were corrected for the sea salt contribution: $\text{nss } X_d = X_d - (X/\text{Na})_{\text{sea-salt}} \times \text{Na}_d$ where subscript d indicates deposition.

Deposition was calculated as the product of concentrations by precipitation amount for WD or by the rinsing volume for DD of individual samples. Weekly or biweekly deposition was added from August 2002 to July 2003 to account for the annual deposition value.

3.3. Identification of African Intrusions

A daily analysis of back trajectories was undertaken based on the HYSPLIT 4.0 dispersion model from the Air Resources Laboratory (www.arl.noaa.gov/ready/hysplit4.html; [44]). Back trajectories were started at 12 UTC (Coordinated Universal Time) and run backwards for 120 hours at each of the sites. For MSY the initial altitude was at 750, 1500 and 2500 m.a.s.l., and for SCO at 100, 1500 and 2500 m.a.s.l. The lowest altitude was established in relation to the altitude of the site (about sea-level at SCO and 700 m at MSY).

Once the back trajectories were obtained, a classification of provenances was undertaken to separate North African trajectories (NAF) from the rest (no-NAF). For that purpose, the following geographical sectors were distinguished: AN: Atlantic (North) advection, ANW: Atlantic (North-Western) advection, AW: Atlantic (Western) advection, ASW: Atlantic (South-Western) advection, EU: European advection; REG: regional recirculation, NAF: North African advection (Figure 2). For the purposes of this study, trajectories from all non African sectors were pooled together in the no-NAF category. Deposition from trajectories in the no-NAF category is compared in this study to deposition from the NAF trajectories. Complementary visual information from satellite images and aerosol maps was obtained to identify African dust outbreaks, based on: (1) satellite images from SeaWiFS and MODIS-Terra, and (2) predictions from aerosol dust concentrations maps of the DREAM (www.bsc.es/projects/earthscience/DREAM), NAAPS (Naval Research Laboratory, www.nrlmry.navy.mil/aerosol), and SKIRON models (www.forecast.uoa.gr; [45]). The meteorological situation was further characterised from synoptic maps obtained from the NOAA-CIRES climate Diagnostic Center (www.cdc.noaa.gov/composites/hour/; [46]).

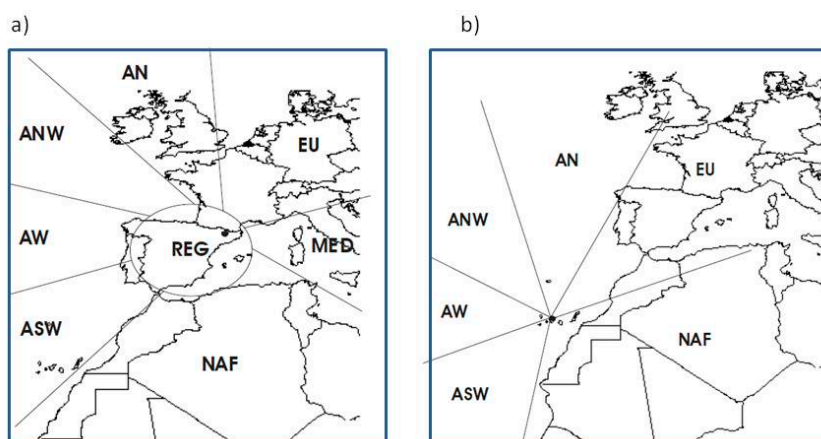


Figure 2. Geographical sectors distinguished for the interpretation of the origin of air masses at Montseny (MSY, (a)) and Santa Cruz de Tenerife (Canary Islands, SCO, (b)). AN: North Atlantic advection, ANW: North-Western Atlantic advection, AW: Western Atlantic advection, ASW: South-Western Atlantic advection, EU: European advection; REG: regional recirculation, NAF: African advection. For the purposes of this study, all non-African sectors were pooled together in the no-NAF category.

For wet samples, the days of rain were first identified and the back trajectories, satellite images, dust models and atmospheric synoptic patterns were evaluated for the rain days. The weekly sample was considered NAF when all the combined evidences indicated an African outbreak during the rainy days. For DD, a week was classified as NAF if at least 3–4 days in the week presented African back trajectories and dust was observed in the satellite images and dust maps.

3.4. Statistics

The seasonal variation of aerosol concentrations and element deposition was modelled with the following Equation:

$$Y_i = a_0 + a B \cos (2\pi/365 t + \phi) \quad (1)$$

where Y_i is the dependent variable, a_0 is a constant, a is the coefficient of the periodic term, ϕ stands for phase in radians and t is the number of days lapsed. This model has two components: one is a constant coefficient (a_0) that gives the mean of the dependent variable for the whole studied period, and the other is a cosine term with a period of 365 days which accounts for the seasonal variation observed in the data. The presence of the cosine term required the use of nonlinear regression techniques (Levenberg-Marquardt algorithm built-in STATISTICA™) to adjust the model to the observations. Concentration and deposition values were previously log-transformed for the cosine model.

To explore ion relationships, Spearman rank correlation coefficients (p) were used due to the non-normal distribution of data.

4. Results and Discussion

4.1. Concentrations in WD and DD

In the study year, average atmospheric particulate levels (TSP) at SCO and MSY were 81 and 25 $\mu\text{g m}^{-3}$, respectively. The higher TSP levels at SCO stem from the site characteristics, such as the important local industrial activities and traffic in and around the Santa Cruz city [47–49], the influence of the marine aerosol due to its position near the sea [50] and, most importantly, a high impact of dust intrusion frequency [18,50]. The site in NE Spain, on the other hand, is further away from the sea (27 km); the closest highway is about 16 km away, and the distance to the nearest city (Barcelona) is 40 km. In addition, African events have a lower incidence: analysis of back trajectories showed that only 15–25% of the days were influenced by African air masses [14,51].

4.1.1. Source of Soluble Ions in WD and DD

Ionic correlations between the measured ions in WD and DD allow an understanding of the ion sources and the reactions involved in the atmosphere before deposition. For DD, correlations may reflect the reactions of the suspended aerosols, but for WD, correlations have a further strong modulator: the amount of precipitation that produces dilution/concentration on the wet content.

DD at SCO, only presented strong correlations ($p > 0.8$) for the pairs $\text{Na}^+ - \text{Cl}^-$, $\text{Na}^+ - \text{Mg}^{2+}$ and $\text{Mg}^{2+} - \text{Cl}^-$, which indicate the marine source in the dryfall, and for $\text{Ca}^{2+} - \text{NO}_3^-$, indicating secondary reactions involving crustal (Ca^{2+}) and anthropogenic pollution (NO_3^-) (Figure 3). Moderate correlations but still significant ($p > 0.6$) were found for alkalinity vs. Ca^{2+} and SO_4^{2-} , indicating a crustal derived component derived from carbonates and gypsum in the dryfall (Figure 3). Secondary reactions between NO_x and HNO_3 with carbonated aerosols have been found to lead to $\text{Ca}(\text{NO}_3)_2$ [52,53]. Other secondary reactions have been identified at SCO, involving coarse NaNO_3 due to the reaction of HNO_3 with marine NaCl , as found in other coastal sites [21]. In addition, coarse CaSO_4 has been found to be the major sulphate phase at SCO during Saharan episodes due to the reaction of SO_2 (or H_2SO_4) from local emissions of ships and a nearby refinery [47,48] with carbonates in the mineral dust. These sulphating and nitrating mechanisms are favoured by: (1) the high concentration of coarse mineral particles with a high specific surface that could act as active reaction surfaces during the Saharan episodes; (2) the relatively high relative humidity measured at

SCO (~63% annual mean value) and (3) and the compression of the marine boundary layer (MBL) during the Saharan episodes, which causes a higher concentration of aerosols in the low levels of the atmosphere [17]. By contrast, DD for NH_4^+ and K^+ did not show significant correlations with the remaining analysed ions or between them. In summary, at SCO dryfall mostly reflects the marine source and the interplay of crustal and anthropogenic emissions that affect the site. However, for WD the picture was quite different at SCO owing to the influence of precipitation amounts on concentrations. Small precipitation events were common (median precipitation = 3.7 mm/event) and these events were highly concentrated, resulting in very strong correlations between all analysed ions (except for NO_3^-) as seen in Figure 2.

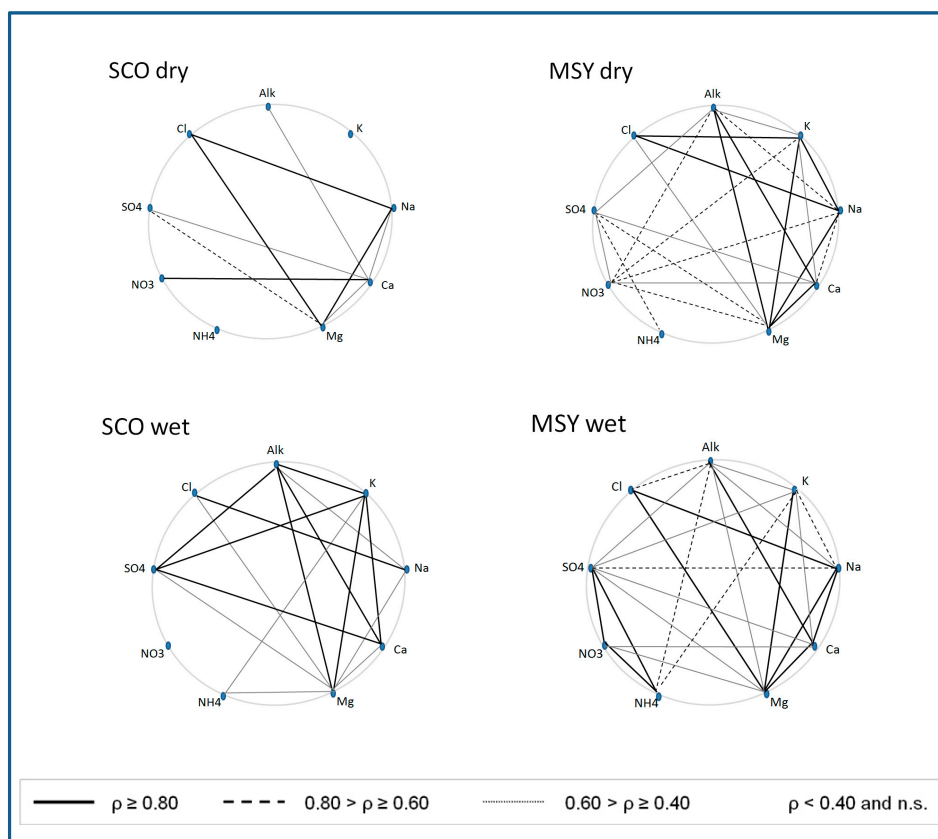


Figure 3. Relationships between ions in wet and dry deposition at the study sites based on Spearman rank correlation coefficients (p).

At MSY, high correlations ($p > 0.8$) in DD were found for the marine ions (Na^+ , Cl^- , and Mg^{2+}) and for crustal derived elements (K^+ , Mg^{2+} , Ca^{2+} , alkalinity; Figure 2). The fact that both Ca^{2+} and alkalinity presented clear peaks during weeks of African intrusions (Figure 3) indicate an important contribution of African dust to DD, similar to what has been found in WD [54,55]. Relatively good correlations ($0.6 > p > 0.8$) were found between NO_3^- and major cations (Mg^{2+} , K^+ , Na^+) and for the pairs $\text{NH}_4^+ - \text{SO}_4^{2-}$, indicating the formation of secondary inorganic aerosols. Lower correlations but still significant were found for the pairs $\text{Ca}^{2+} - \text{SO}_4^{2-}$ and $\text{NO}_3^- - \text{SO}_4^{2-}$. Thus, dryfall at MSY was influenced by marine aerosols and a clear anthropogenic influence was detected involving NH_4^+ , NO_3^- and SO_4^{2-} . Previous work at MSY has reported that ammonium sulphate could derive from regional pollution having a special prevalence in summer, and ammonium nitrate, from winter local emissions due to its instability at high temperatures [40]. It is also possible that ammonium nitrate and sulphate aerosols at MSY originated from regional-scale gaseous precursors [40]. Due to their small size, these particles tend to travel for long distances, so that they could originate from distant sources

and recirculate in the western Mediterranean basin [56]. For WD, the marine and crustal components were also clearly defined with correlations coefficients greater than 0.80 (Figure 3). In general, dilution of all ions with precipitation resulted in high correlations between most ion pairs, the exception being NH_4^+ which only had strong correlations with NO_3^- and SO_4^{2-} ($r > 0.8$), attesting to the inclusion of ammonium nitrate and sulphate aerosols in precipitation, and with K^+ and alkalinity ($p > 0.6$; Figure 3).

Various studies of aerosols and deposition in Southern Europe coastal sites have reported a departure of the Na^+/Cl^- ratio from the marine ratio (0.86 in terms of equivalents; Drever 1982). In general, a deficit of Cl^- was observed [12,57,58]. This deficit would result from the reaction of NaCl with HNO_3 , to produce $\text{NaNO}_3 + \text{HCl(g)}$, with the latter evaporating. This process leads to Cl^- being exchanged for NO_3^- ; thus, the Na^+/Cl^- ratio would become higher than the marine ratio but the $\text{Na}^+/(\text{Cl}^- + \text{NO}_3^-)$ ratio should approach 0.86. At a site in Sierra Nevada (southern Spain), this substitution was found for WD but not for DD, suggesting the interplay of different exchange reactions under dry and wet conditions [12]. At the coastal SCO site, Na^+/Cl^- exceeded the marine ratio (0.92 and 1.02, for WD and DD, respectively) and the incorporation NO_3^- reduced them to values close to the marine ratio $\text{Na}^+/(\text{Cl}^- + \text{NO}_3^-) = 0.79$ and 0.89 for WD and DD). At SCO, DD behaved similar to WD, indicating that at this site there was a sufficient HNO_3 source for the reaction. On the contrary, at MSY, the Na^+/Cl^- ratio was close to the marine ratio for both deposition modes (0.87 and 0.86 for WD and DD respectively) and strongly decreased when including NO_3^- in the denominator, indicating the lack of reaction between sea salt and acid nitric at this site. This different behaviour is consistent with the suggestion that the abovementioned reaction leading to a Cl^- deficit from the marine ratio is linked to arid conditions [12].

4.1.2. Wet and Dry Chemical Composition at Both Sites

The ratios of the mean concentrations between sites (SCO/MSY) are presented here to compare the contents for the analysed ions in WD and DD at both sites (Table 1). These ratios were higher than 1 for all ions, except for NH_4^+ and nssMg^{2+} , while for NO_3^- the ratio was close to 1. Ions of marine origin (Na^+ , Cl^- and Mg^{2+}) showed the highest SCO/MSY ratios (12.7–16.0 Table 1), indicating the impact of the sea spray at the coastal city of Santa Cruz. However, for crustal Mg^{2+} (nssMg^{2+} calculated by subtracting the marine contribution from Mg^{2+}), the ratio SCO/MSY decreased to 0.1–0.2, revealing that most of the Mg^{2+} deposited at SCO is from marine origin, while at MSY the crustal contribution dominated. For other crustal-derived ions, such as Ca^{2+} , K^+ and alkalinity, the ratio SCO/MSY ranged between 2.4–4.6 for wet and 1.6–2.7 for DD. Higher concentrations of crustal-derived elements at SCO are consistent with the higher frequency of African intrusions and higher particulate loads in the atmosphere of Tenerife [16,18,29]. While the SCO/MSY ratio is similar for nssCa^{2+} and nssMg^{2+} in WD and DD (around 2.4 and 0.1 respectively, Table 1), for alkalinity and K this ratio is higher in wet than in DD. This is due to the relatively low alkalinity and K concentrations in WD at MSY.

Table 1. Mean concentrations of major soluble elements in wet and dry deposition (microequivalent L^{-1}) and ratios between the Montseny (MSY) and Santa Cruz de Tenerife (SCO) sites. For wet deposition, concentrations have been weighted by precipitation volume (VWM). For dry deposition the values correspond to arithmetic means, since a fixed volume for rinsing (250 mL) has been used. nss = non sea salt concentration.

Variable	MSY	SCO	SCO/MSY	MSY	SCO	SCO/MSY
	Wet Deposition			Dry Deposition		
Prec. (mm)	881	134	0.2			
Cond.	17.1	89.1	5.2	25.9	111	4.3
Na^+	22.9	357.0	15.6	20.5	329	16.0
K^+	3.5	15.0	4.3	16.5	25.7	1.6
Ca^{2+}	108	257.0	2.4	201	498	2.5
nssCa^{2+}	107	242.7	2.3	192	491	2.6

Table 1. Cont.

Variable	MSY	SCO	SCO/MSY	MSY	SCO	SCO/MSY
	Wet Deposition			Dry Deposition		
Mg ²⁺	9.3	82.0	8.8	22.1	76.3	3.5
nssMg ²⁺	4.1	1.0	0.2	17.4	1.6	0.1
NH ₄ ⁺	31.8	19.6	0.6	29.7	10.1	0.3
NO ₃ [−]	22.7	24.0	1.1	34.8	39.1	1.1
SO ₄ ^{2−}	33.0	130.0	3.9	34.3	152	4.4
nssSO ₄ ^{2−}	30.2	87.2	2.9	31.8	114.2	3.6
Cl [−]	27.1	430	15.9	29.5	376	12.7
Alk.	43.9	204.0	4.6	152	407	2.7

4.2. Deposition Fluxes

Total deposition fluxes for the insoluble particulate matter were 17.1 and 5.4 g m^{−2} year^{−1} for SCO and MSY, respectively. At SCO, particulate matter deposition occurred mostly in the dry form (60%, Table 2), while at MSY, most of the particulate matter flux was in the wet mode (Table 2).

For marine ions, total (wet + dry) Cl[−] and Na⁺ deposition fluxes were ~4-fold higher at SCO compared to MSY (Table 2). At SCO, WD and DD contributed similarly, while at MSY, deposition of marine ions occurred mostly in the wet mode (82% and 85% for Cl[−] and Na⁺, respectively, Table 2). Alkalinity (here expressed as HCO₃−C) and SO₄−S presented a similar total deposition between sites, while for K⁺, Ca²⁺, NH₄−N and NO₃−N, total deposition was higher at MSY (Table 2). Most of the deposition at SCO occurred as DD, except for marine elements and NH₄−N. At MSY, WD predominated, with K⁺ showing the lowest WD contribution (Table 2).

Table 2. Wet, dry and total (wet + dry) deposition fluxes at Montseny (MSY) and Santa Cruz de Tenerife (SCO) in kg ha^{−1} year^{−1} (except for particulate matter (PM) in g m^{−2} year^{−1}), and percent of wet relative to total (wet + dry) deposition.

Variable	MSY Wet	MSY Dry	MSY Total	MSY % Wet/Tot	SCO Wet	SCO Dry	SCO Total	SCO % Wet/Tot
PM	3.3	2.1	5.4	61.1	5.1	12.0	17.1	29.8
Na ⁺	4.6	0.83	5.43	84.7	11	9.55	20.5	53.5
K ⁺	1.2	1.13	2.33	51.5	0.79	1.27	2.06	38.3
Ca ²⁺	19.1	7.12	26.2	72.8	6.9	12.6	19.5	35.4
Mg ²⁺	0.98	0.47	1.45	67.6	1.33	1.17	2.5	53.2
NH ₄ −N	3.73	0.73	4.46	83.6	0.36	0.18	0.54	66.7
NO ₃ −N	2.8	0.86	3.66	76.5	0.45	0.7	1.15	39.1
SO ₄ −S	4.65	0.97	5.62	82.7	2.79	3.07	5.86	47.6
Cl [−]	8.46	1.84	10.3	82.1	20.4	16.8	37.2	54.8
HCO ₃ −C	4.56	3.21	7.77	58.7	3.27	6.16	9.43	34.7

The difference in the ratios of wet to total deposition for the analysed ions (range: 60–85% except K⁺ at MSY, and 35–55% at SCO, except for NH₄⁺) illustrates the dependence of deposition fluxes on the particular precipitation regime of the two sites and their local atmospheric load, which is highly influenced by African intrusions at SCO. Rain is an effective vehicle for deposition and delivers elements either by scavenging atmospheric particles and gases from a local origin (washout mechanism) or by delivering particles from longer distances that have travelled incorporated into the clouds (rainout mechanism) [59]. As rain becomes scarce, dryfall takes a more prominent role, accounting for most of the deposition of coarse aerosols, such as those derived from mineral dust. This is the case for SCO, where most of the crustal elements were delivered in the dry mode. The fact that NO₃−N and SO₄−S deposition was also dominant in the dry mode at this site confirms the previous

interpretation of secondary aerosol formation from the reaction of crustal-derived material with local industrial and traffic emissions, which are important at SCO [17,49].

4.2.1. Seasonality of Deposition Fluxes

At SCO, atmospheric particles (PM₁₀) presented lower levels in winter (data not shown); however the seasonal model did not explain the temporal variation of DD (variance explained <5%). SCO is significantly influenced by the presence of African air masses, and high DD fluxes were observed during African episodes. In winter, low pressures over the Atlantic close to the Canary Islands cause the simultaneous appearance of Saharan dust (raised by the right branch of these lows) and rains, resulting in a maximum frequency of WD episodes at SCO. However, during our period of study, WD was mostly conditioned by a single rain event on 19 December 2002 (85.5 mm, Figure 4; upper panel right). This event, originating from the SW Atlantic Ocean, accounted for 64% of annual precipitation and 30% of the annual WD flux of K^+ , Na^+ , Mg^{2+} , SO_4^{2-} , Cl^- , and 46% and 58% for NO_3^- and NH_4^+ , respectively. In summary, at SCO, the temporal variation of DD is highly conditioned by the arrival of African intrusions, while the WD flux is strongly dependent on the occurrence of rain events.

At MSY, TSP levels and particulate matter WD and DD presented a general pattern of low values in winter and high values in summer (data not shown). Soluble elements in DD showed a similar temporal variation, with higher concentrations in summer (Figure 3; lower panel left). The seasonal cosine model (Equation (1)) explained between 15% and 30% of this seasonal variability, except for NO_3-N . By contrast, the variability of WD was not explained by the cosine seasonal model (except for Ca, with 19% of the variability explained). Variability in the wet mode was greatly influenced by the episodic occurrence of African rain events (Figure 4; upper panel left).

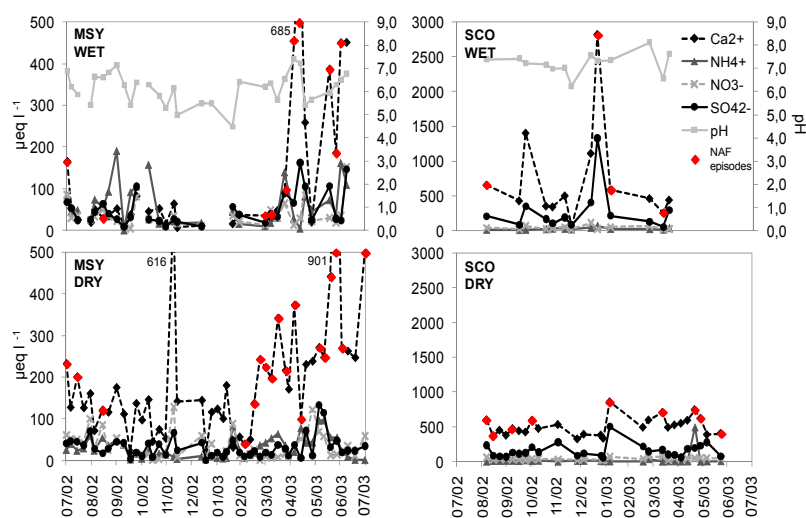


Figure 4. Temporal variation of ion concentrations (Ca^{2+} , NH_4^+ , NO_3^- , SO_4^{2-}) and pH in wet and DD. North African episodes (NAF) are highlighted (red diamonds). MSY = Montseny; SCO = Santa Cruz de Tenerife.

At MSY, in autumn-winter the site is above the mixing layer and connected to the cleaner free troposphere. Furthermore, in winter, frequent rain-laden Atlantic advections occur that clean the atmosphere of pollutants [37,60]. On the other hand, in spring-summer the MBL increases in altitude so that the site is within the mixing layer and is affected by local/regional pollutants that build up during long dry spells, thus explaining the higher summer particulate matter levels and element deposition. Although African dust outbreaks to the West Mediterranean tend to occur in spring-summer [36,40].

WD of African dust is highly dependent on sporadic dust uplifts combined with frontal systems that cross the Mediterranean from west to east which often occur in autumn and spring [51].

4.2.2. African Dust in WD and DD

To evaluate the contribution of African dust in each location, the fluxes deposited during North African dust intrusions (NAF) were distinguished from samples not affected by African air masses (No-NAF). In Table 3 the number of samples pertaining to each category is presented. At SCO, about half of the samples during the study period corresponded to air masses from an African provenance either in WD or DD, while at MSY the African events only accounted for 29% (WD) and 25% (DD) of the total samples. NAF events delivered 69% (WD) and 64% (DD) of insoluble particulate matter at SCO. However, at MSY, NAF accounted for 91% of wet particulate matter deposition and 70% of its DD (Table 4). Thus, African dust was responsible of most of the insoluble particulate matter deposition at all sites, and was particularly important (91%) for WD at MSY. Particulate matter deposition (sum of wet + dry) during NAF events was more than double at SCO than at MSY (11.2 vs. 4.5 g m⁻² year⁻¹; Table 4). Since particulate matter in WD during African events was similar between the sites (3 g m⁻² year⁻¹), a higher DD flux at SCO during NAF intrusions (7.7 at SCO vs. 1.4 g m⁻² year⁻¹ at MSY) explained the observed difference. No-NAF episodes also delivered an important particulate matter deposition flux at SCO, most of it (73%) as DD (Table 4). Therefore, NAF episodes had an important role in particulate matter deposition at the two sites: the site closer to the African source received a higher NAF deposition flux, 70% as DD; by contrast, the distant site received about half P particulate matter deposition in NAF events, most of it in the wet form (PM in NAF events accounted for 55% of total (wet + dry) particulate matter deposition).

Table 3. Number of events in the Montseny (MSY) and Santa Cruz de Tenerife (SCO) sites and provenance category. NAF = samples corresponding to air masses of North African provenance; no-NAF = samples from air masses corresponding to other provenances.

Number Samples	SCO		MSY	
	Wet	Dry	Wet	Dry
NAF	7	15	9	12
No-NAF	6	11	22	35
Total	13	26	31	47
% NAF	54	58	29	25

Table 4. Deposition of particulate matter (PM, in g m⁻² year⁻¹) in the Montseny (MSY) and Santa Cruz de Tenerife (SCO) sites and provenance category. The percentages of dry to wet + dry deposition and %NAF deposition are also shown. NAF = samples corresponding to air masses of North African provenance; no-NAF = samples corresponding to air masses from other provenances.

Particulate Matter	SCO				MSY			
	Wet	Dry	W + D	% D/W + D	Wet	Dry	W + D	% D/W + D
NAF	3.5	7.7	11.2	69	3.0	1.5	4.5	33
No-NAF	1.6	4.3	5.9	73	0.3	0.7	1.0	70
Total Annual	5.1	12	17.1	70	3.3	2.2	5.5	40
% NAF	69	64			91	70		

Deposition of marine-derived ions was much higher at SCO than MSY, a difference particularly striking for DD (Figure 5). For WD, the difference between sites was mostly due to no-NAF samples, since the amounts deposited during NAF events were very similar between sites (for Cl⁻: 5.5 and 5.4 kg ha⁻² year⁻¹ and for Na⁺: 3.4 and 3.0 kg ha⁻² year⁻¹ at SCO and MSY, respectively). At SCO, DD during NAF events was the most prominent flux for crustal elements (here exemplified with

Ca^{2+} and $\text{HCO}_3\text{-C}$; Figure 5), while at MSY, WD during NAF events was important, accounting for 45% and 39% for Ca^{2+} and $\text{HCO}_3\text{-C}$ of total wet + dry deposition, respectively (Figure 5). This is consistent with the fact that African air masses at SCO transport coarse dust particle that tend to sediment gravitationally. Instead, at MSY, African dust is mostly delivered through the arrival of perturbations from the western Mediterranean that produce important rain events and that are heavily dust laden [42,51].

Sulphate deposition amounts at SCO were similar in both deposition modes (2.8 and $3.1 \text{ kg ha}^{-1} \text{ year}^{-1}$ $\text{SO}_4\text{-S}$ for WD and DD, respectively; Figure 5), but the African contribution was higher in the dry mode (61% vs. 40%). Dust from the Sahara has been found to produce secondary sulphates that are mostly comprised in the coarser modes and may contribute to dryfall at this site [17,50]. On the other hand, at MSY, $\text{SO}_4\text{-S}$ WD about quintupled DD (4.6 vs. $1.0 \text{ kg ha}^{-2} \text{ year}^{-1}$) and NAF events contributed 40% of WD but only 24% of dry $\text{SO}_4\text{-S}$ deposition.

The deposition patterns of nitrogen compounds were strikingly different from the abovementioned elements: MSY received higher deposition amounts than SCO for $\text{NO}_3\text{-N}$ and $\text{NH}_4\text{-N}$, mostly in the wet mode (Figure 6). NAF events had a small contribution to the total deposition amounts at MSY, while at SCO NAF events significantly contributed to DD of $\text{NO}_3\text{-N}$.

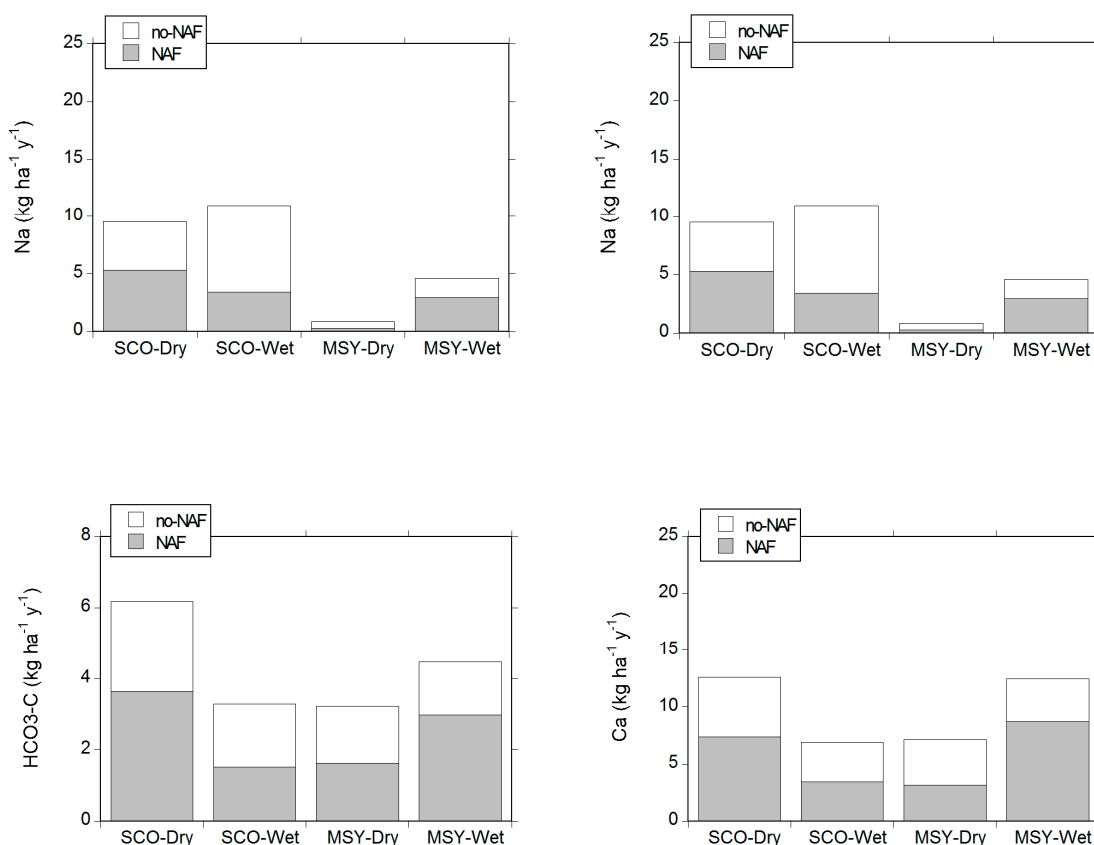


Figure 5. Deposition fluxes (in $\text{kg ha}^{-1} \text{ year}^{-1}$) of dry and wet deposition at the two study sites (SCO = Santa Cruz de Tenerife; MSY = Montseny) for marine elements (Na^+ , Cl^-) and crustal-derived elements ($\text{HCO}_3\text{-C}$ and Ca^{2+}). Deposition during African (NAF) and non-African events (no-NAF) is indicated.

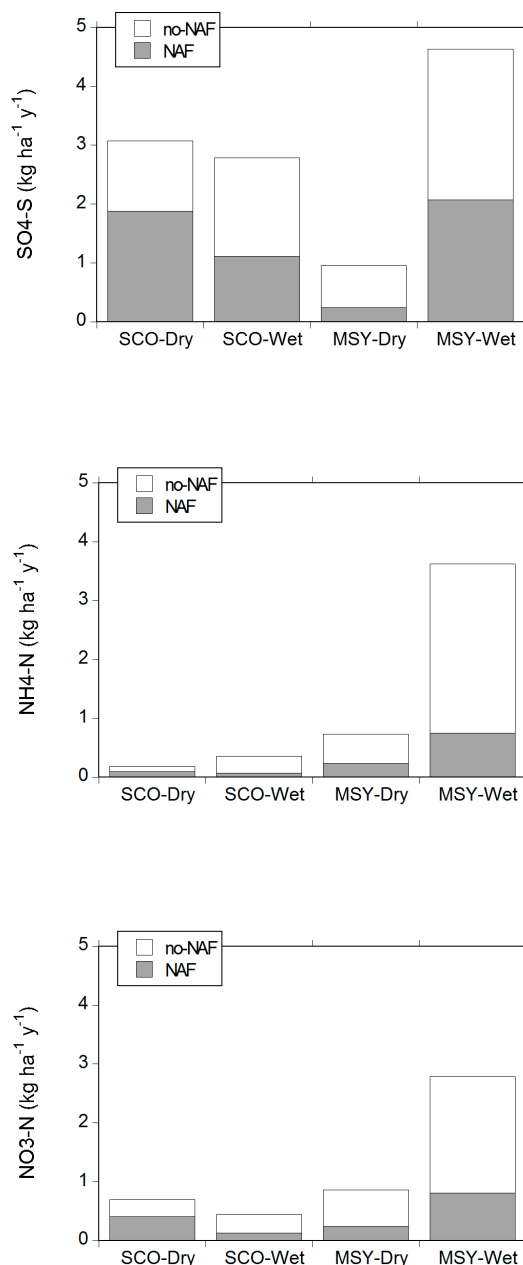


Figure 6. Deposition fluxes (in $\text{kg ha}^{-1} \text{ year}^{-1}$) of dry and wet deposition at the two study sites (SCO = Santa Cruz de Tenerife; MSY = Montseny for pollution-derived elements. Deposition during African (NAF) and non-African events (no-NAF) is indicated.

Despite the fact that samples from no-NAF events dominated in MSY, it is worth noticing that WD of $\text{SO}_4\text{-S}$, $\text{NO}_3\text{-N}$ and $\text{NH}_4\text{-N}$ during NAF events at this distant site was higher than NAF deposition at the site close to Africa, either in the wet or dry mode. This fact suggests that mineral dust acts as a surface of pollutant reaction, the surface being coated with ammonium, sulphate and nitrate ions as observed in mineral dust aerosols crossing polluted regions in east Asia [61] and other regions [53]. Furthermore, it has been proposed that desert dust is transformed by these reactions, changing from a hydrophobic to a hydrophilic nature that favours the formation of CCN, thus enhancing WD [62]. In line with this hypothesis, we did observe higher $\text{SO}_4\text{-S}$, $\text{NO}_3\text{-N}$ and $\text{NH}_4\text{-N}$ in wet NAF events at the distant site.

On the other hand, the predominant trade winds in the Canary Islands may carry away local emissions causing the deposition of these pollutants to occur at distant sites in the ocean. At SCO, N deposition (the sum of $\text{NO}_3\text{-N}$ and $\text{NH}_4\text{-N}$) in the wet and dry forms amounted only $1.7 \text{ kg N ha}^{-1} \text{ year}^{-1}$. This is a very low N deposition flux (likely underestimated because of the underrepresentation of fine aerosols in the DD method used) which ranks within the lowest values reported for Spanish sites [63]. This indicates that precursor emissions in Santa Cruz and surrounding industrial areas have a small impact in N deposition at this site.

5. Conclusions

This study addresses the effect of distance to the African coast and site meteorology on total deposition of soluble elements and particulate matter, distinguishing between deposition in the dry and wet modes and specifically accounting for the African contribution. Results corroborate the hypothesis that DD near dust sources overcomes WD for coarse particles while this predominance weakens as distance from Africa increases. In this sense, total deposition for insoluble particulate matter was more than 3-fold higher at the site in front of the African coast. On the other hand, for the soluble fraction of crustal elements, the particular meteorology of the sites had a stronger role related to the fact that rainfall scavenging of aerosols is a very effective process to deliver particles to the surface. Owing to this, deposition of soluble elements of crustal origin (e.g., Ca^{2+} , K^+) was higher at the wetter, distant site in the Iberian Peninsula. In the NE of the Iberian Peninsula, African provenances account for a low percentage of the rain events but they cause the arrival of heavily dust-loaded fronts. In this study, rain events from North Africa accounted for most (75%) WD fluxes of crustal elements at the Iberian Peninsula site. On the other hand, at the more arid site in the Canary Islands, dry deposition dominated, and half of it corresponded to African provenances. All in all, both sites received a similar contribution of soluble crustal elements from Africa (e.g., $\sim 12 \text{ kg ha}^{-2} \text{ year}^{-1}$ for Ca^{2+}) but the dominance shifted from WD to DD depending on the particular meteorology of the sites.

For anthropogenic derived elements, it is worth noticing the very low $\text{NO}_3\text{-N}$ and $\text{NH}_4\text{-N}$ deposition values in the Canary Islands, both in WD and DD, suggesting that trade winds from the NE carry away local NO_y and NH_3 emissions and that little pollution of these compounds is acquired from North Africa. Conversely, at the site in the Iberian Peninsula, deposition of $\text{SO}_4\text{-S}$, $\text{NO}_3\text{-N}$ and $\text{NH}_4\text{-N}$ was higher, mostly contributed by WD. For these elements, the North African share in deposition increased with distance, suggesting that mineral dust acts as a surface of pollutant reaction, being coated with ammonium, sulphate and nitrate ions as the dust plume travels from North Africa to the Western Mediterranean and reacts with pollutants encountered during this trajectory.

Acknowledgments: We acknowledge the financial support from the Spanish Government (CGL2005-07543-CLI, CGL2009-13188-C03-01, CSD2008-00040-Consolider Montes grants and the “Subprograma MICINN-PTA” funded by the European Social Fund). The Global Atmospheric Watch program at the Air Quality Research Observatory at Santa Cruz de Tenerife has been funded by AEMET. The IDAEA group acknowledges the financial support of the Generalitat de Catalunya (AGAUR 2014 SGR33 and the DGQA).

Author Contributions: Xavier Querol, Emilio Cuevas, Andrés Alastuey and Anna Avila conceived and designed the experiments; Sonia Castillo performed the experimental tasks and analyzed the data; Sonia Castillo and Anna Avila wrote the paper; all authors revised the article.

Conflicts of Interest: The authors declare no conflict of interest.

References

1. Lequy, E.; Conil, S.; Turpault, M.P. Impacts of Aeolian dust deposition on European forest sustainability: A review. *For. Ecol. Manag.* **2012**, *267*, 240–252.
2. Schulz, M.; Prospero, J.M.; Baker, A.R.; Dentener, F.; Ickes, L.; Liss, P.S.; Mahowald, N.M.; Nickovic, S.; García-Pando, C.P.; Rodríguez, S.; et al. Atmospheric Transport and Deposition of Mineral Dust to the Ocean: Implications for Research Needs. *Environ. Sci. Technol.* **2012**, *46*, 10390–10404. [[CrossRef](#)] [[PubMed](#)]

3. Seinfeld, J.H.; Pandis, S.N. *Atmospheric Chemistry and Physics. Air Pollution to Climate Change*; John Wiley and Sons: New York, NY, USA, 1998.
4. Lovett, G.M. Atmospheric deposition of nutrients and pollutants in North America: An ecological perspective. *Ecol. Appl.* **1994**, *4*, 629–650. [[CrossRef](#)]
5. Mészáros, E. *Fundamentals of Atmospheric Aerosol Chemistry*; Akadémiai Kiado: Budapest, Hungary, 1999.
6. Wesely, M. A review of the current status of knowledge on dry deposition. *Atmos. Environ.* **2000**, *34*, 2261–2282. [[CrossRef](#)]
7. Kubilay, N.; Nickovic, S.; Moulin, C.; Dulac, F. An illustration of the transport and deposition of mineral dust onto the eastern Mediterranean. *Atmos. Environ.* **2000**, *34*, 1293–1303. [[CrossRef](#)]
8. Markaki, Z.; Oikonomou, K.; Kocak, M.; Kouvarakis, G.; Chaniotaki, A.; Kubilay, N.; Mihalopoulos, N. Atmospheric deposition of inorganic phosphorus in the Levantine Basin, eastern Mediterranean: Spatial and temporal variability and its role in seawater productivity. *Limnol. Oceanogr.* **2003**, *48*, 1557–1568. [[CrossRef](#)]
9. Guieu, C.; Loye-Pilot, M.D.; Benyahya, L.; Dufour, A. Spatial variability of atmospheric fluxes of metals (Al, Fe, Cd, Zn and Pb) and phosphorus over the whole Mediterranean from a one-year monitoring experiment: Biogeochemical implications. *Mar. Chem.* **2010**, *120*, 164–178. [[CrossRef](#)]
10. Izquierdo, R.; Benítez-Nelson, C.R.; Masqué, P.; Castillo, S.; Alastuey, A.; Àvila, A. Atmospheric phosphorus deposition in a near-coastal rural site in the NE Iberian Peninsula and its role in marine productivity. *Atmos. Environ.* **2012**, *49*, 361–370. [[CrossRef](#)]
11. Morales-Baquero, R.; Pulido-Villena, E.; Reche, I. Atmospheric inputs of phosphorus and nitrogen to the southwest Mediterranean region: Biogeochemical responses of high mountain lakes. *Limnol. Oceanogr.* **2006**, *51*, 830–837. [[CrossRef](#)]
12. Morales-Baquero, R.; Pulido-Villena, E.; Reche, I. Chemical signature of saharan dust on dry and wet atmospheric deposition in the south-western mediterranean region. *Tellus Ser. B Chem. Phys. Meteorol.* **2013**, *65*, 1–11. [[CrossRef](#)]
13. Escudero, M.; Querol, X.; Ávila, A.; Cuevas, E. Origin of the exceedances of the European daily PM limit value in regional background areas of Spain. *Atmos. Environ.* **2007**, *41*, 730–744. [[CrossRef](#)]
14. Izquierdo, R.; Avila, A.; Alarcón, M. Trajectory statistical analysis of atmospheric transport patterns and trends in precipitation chemistry of a rural site in NE Spain in 1984–2009. *Atmos. Environ.* **2012**, *61*, 400–408. [[CrossRef](#)]
15. Pey, J.; Alastuey, A.; Querol, X. PM10 and PM2.5 sources at an insular location in the western mediterranean by using source apportionment techniques. *Sci. Total Environ.* **2013**, *456–457*, 267–277. [[CrossRef](#)] [[PubMed](#)]
16. Viana, M.; Querol, X.; Alastuey, A.; Cuevas, E.; Rodríguez, S. Influence of African dust on the levels of atmospheric particulates in the Canary Islands air quality network. *Atmos. Environ.* **2002**, *36*, 5861–5875. [[CrossRef](#)]
17. Alastuey, A.; Querol, X.; Castillo, S.; Escudero, M.; Avila, A.; Cuevas, E.; Torres, C.; Romero, P.M.; Exposito, F.; García, O.; et al. Characterisation of TSP and PM2.5 at Izaña and Sta. Cruz de Tenerife (Canary Islands, Spain) during a Saharan Dust Episode (July 2002). *Atmos. Environ.* **2005**, *39*, 4715–4728. [[CrossRef](#)]
18. Alonso-Pérez, S.; Cuevas, E.; Querol, X. Objective identification of synoptic meteorological patterns favouring African dust intrusions into the marine boundary layer of the subtropical eastern north Atlantic region. *Meteorol. Atmos. Phys.* **2011**, *113*, 109–124. [[CrossRef](#)]
19. Sicard, M.; Barragan, R.; Dulac, F.; Alados-Arboledas, L.; Mallet, M. Aerosol optical, microphysical and radiative properties at regional background insular sites in the western Mediterranean. *Atmos. Chem. Phys.* **2016**, *16*, 12177–12203. [[CrossRef](#)]
20. Camarero, L.; Catalan, J. Variability in the chemistry of precipitation in the Pyrenees (NE Spain): dominance of storm origin and lack of altitude influence. *J. Geophys. Res.* **1996**, *101*, 29491–29498. [[CrossRef](#)]
21. Pandolfi, M.; Alastuey, A.; Reche, C.; Castro, I.; Shatalov, V.; Querol, X. Trends analysis of PM source contributions and chemical tracers in NE Spain during 2004–2014: A multi-exponential approach. *Atmos. Chem. Phys.* **2016**, *16*, 11787–11805. [[CrossRef](#)]
22. Izquierdo, R.; Avila, A. Comparison of collection methods to determine atmospheric deposition in a rural Mediterranean site (NE Spain). *J. Atmos. Chem.* **2012**, *69*, 351–368. [[CrossRef](#)]
23. Dueñas, C.; Fernández, M.C.; Gordo, E.; Cañete, S.; Pérez, M. Chemical and radioactive composition of bulk deposition in Málaga (Spain). *Atmos. Environ.* **2012**, *62*, 1–8. [[CrossRef](#)]
24. López-García, P.; Gelado-Caballero, M.D.; Santana-Castellano, D.; Suárez de Tangil, M.; Collado-Sánchez, C.; Hernández-Brito, J.J. A three-year time-series of dust deposition flux measurements in Gran Canaria, Spain: A comparison of wet and dry surface deposition samplers. *Atmos. Environ.* **2013**, *79*, 689–694. [[CrossRef](#)]

25. Dolske, D.A.; Gatz, D.F. A field intercomparison of methods for the measurement of particle and gas dry deposition. *J. Geophys. Res.* **1985**, *90*, 2076–2084. [[CrossRef](#)]
26. Guerzoni, S.; Quarantotto, G.; Molinaroli, E.; Rampazzo, G. More data on source signature and seasonal fluxes to the Central Mediterranean Sea of aerosol dust originated in desert areas. *Water Pollut. Res. Rep.* **1995**, *32*, 267–274.
27. Díaz, A.M.; Díaz, J.P.; Expósito, F.J.; Hernández-Leal, P.A.; Savoie, D.; Querol, X. Air masses and aerosols chemical components in the free troposphere at the subtropical Northeast Atlantic region. *J. Atmos. Chem.* **2006**, *53*, 63–90. [[CrossRef](#)]
28. Gangoiti, G.; Alonso, L.; Navazo, M.; Antonio Garcia, J.; Millán, M.M. North African soil dust and European pollution transport to America during the warm season: Hidden links shown by a passive tracer simulation. *J. Geophys. Res. Atmos.* **2006**, *111*, 1–25. [[CrossRef](#)]
29. Rodríguez, S.; Cuevas, E.; Prospero, J.M.; Alastuey, A.; Querol, X.; López-Solano, J.; García, M.I.; Alonso-Pérez, S. Modulation of Saharan dust export by the North African dipole. *Atmos. Chem. Phys.* **2015**, *15*, 7471–7486. [[CrossRef](#)]
30. Gkikas, A.; Hatzianastassiou, N.; Mihalopoulos, N.; Katsoulis, V.; Kazadzis, S.; Pey, J.; Querol, X.; Torres, O. The regime of intense desert dust episodes in the Mediterranean based on contemporary satellite observations and ground measurements. *Atmos. Chem. Phys.* **2013**, *13*, 12135–12154. [[CrossRef](#)]
31. Alonso-Pérez, S.; Cuevas, E.; Querol, X.; Viana, M.; Guerra, J.C. Impact of the Saharan dust outbreaks on the ambient levels of total suspended particles (TSP) in the marine boundary layer (MBL) of the Subtropical Eastern North Atlantic Ocean. *Atmos. Environ.* **2007**, *41*, 9468–9480. [[CrossRef](#)]
32. Font, I. *El tiempo Atmosférico en las Islas Canarias, Serie A*; INM: Madrid, Spain, 1956.
33. Carrillo, J.; Guerra, J.C.; Cuevas, E.; Barrancos, J. Characterization of the Marine Boundary Layer and the Trade-Wind Inversion over the Sub-tropical North Atlantic. *Bound.-Layer Meteorol.* **2016**, *158*, 311–330. [[CrossRef](#)]
34. Moulin, C.; Lambert, C.E.; Dulac, F.; Dayan, U. Control of atmospheric export of dust from North Africa by the North Atlantic Oscillation. *Nature* **1997**, *387*, 691–694.
35. Papayannis, A.; Amiridis, V.; Mona, L.; Tsaknakis, G.; Balis, D.; Bösenberg, J.; Chaikovski, A.; De Tomasi, F.; Grigorov, I.; Mattis, I.; et al. Systematic lidar observations of Saharan dust over Europe in the frame of EARLINET (2000–2002). *J. Geophys. Res. Atmos.* **2008**, *113*, 1–17. [[CrossRef](#)]
36. Pérez, N.; Pey, J.; Castillo, S.; Viana, M.M.; Alastuey, A.; Querol, X. Interpretation of the variability of levels of regional background aerosols in the Western Mediterranean. *Sci. Total Environ.* **2008**, *407*, 527–540. [[CrossRef](#)] [[PubMed](#)]
37. Cusack, M.; Alastuey, A.; Pérez, N.; Pey, J.; Querol, X. Trends of particulate matter (PM 2.5) and chemical composition at a regional background site in the Western Mediterranean over the last nine years (2002–2010). *Atmos. Chem. Phys.* **2012**, *12*, 8341–8357. [[CrossRef](#)]
38. Millan, M.; Salvador, R.; Mantilla, E.; Kallos, G. Photo-oxidant dynamics in the Mediterranean basin in summer. Results from European research projects. *J. Geophys. Res.* **1999**, *102*, 8811–8823. [[CrossRef](#)]
39. Rodríguez, S.; Querol, X.; Alastuey, A.; Mantilla, E. Origin of high summer PM10 and TSP concentrations at rural sites in Eastern Spain. *Atmos. Environ.* **2002**, *36*, 3101–3112. [[CrossRef](#)]
40. Pey, J.; Pérez, N.; Castillo, S.; Viana, M.; Moreno, T.; Pandolfi, M.; López-Sebastián, J.M.; Alastuey, A.; Querol, X. Geochemistry of regional background aerosols in the Western Mediterranean. *Atmos. Res.* **2009**, *94*, 422–435. [[CrossRef](#)]
41. Querol, X.; Pey, J.; Pandolfi, M.; Alastuey, A.; Cusack, M.; Pérez, N.; Moreno, T.; Viana, M.; Mihalopoulos, N.; Kallos, G.; et al. African dust contributions to mean ambient PM10 mass-levels across the Mediterranean Basin. *Atmos. Environ.* **2009**, *43*, 4266–4277. [[CrossRef](#)]
42. Avila, A.; Queralt-Mitjans, I.; Alarcón, M. Mineralogical composition of African dust delivered by red rains over northeastern Spain. *J. Geophys. Res.* **1997**, *102*, 21977–21996. [[CrossRef](#)]
43. Golterman, H.L.; Clymo, R.S.; Ohnstad, M.A. *Methods for Physical and Chemical Analysis of Fresh Waters*; Blackwell Scientific Publications: Oxford, UK, 1978.
44. Draxler, R.R.; Rolph, G.D. HYSPLIT (Hybrid Single-Particle Lagrangian Integrated Trajectory) Model. Access via NOAA, ARI, READY. Available online: <http://ready.arl.noaa.gov/HYSPLIT.php> (accessed on 30 September 2005).

45. Kallos, G.; Kotroni, V.; Lagouvardos, K. The regional weather forecasting system SKIRON. In *An Overview Symposium on Regional Weather Prediction on Parallel Computer Environments*; University of Athens: Athens, Greece, 1997; pp. 209–233.
46. Kalnay, E.; Kanamitsu, M.; Kistler, R.; Collin, W.; Deaven, D.; Gandin, L.; Iredell, M.; Saha, S.; White, G.; Wollen, J.; et al. The NCEP/NCAR 40-year reanalysis project. *Bull. Am. Meteorol. Soc.* **1996**, *77*, 437–471. [[CrossRef](#)]
47. Rodríguez, S.; Cuevas, E.; González, Y.; Ramos, R.; Romero, P.M.; Pérez, N.; Querol, X.; Alastuey, A. Influence of sea breeze circulation and road traffic emissions on the relationship between particle number, black carbon, PM₁, PM_{2.5} and PM_{2.5-10} concentrations in a coastal city. *Atmos. Environ.* **2008**, *42*, 6523–6534. [[CrossRef](#)]
48. González, Y.; Rodríguez, S. A comparative study on the ultrafine particle episodes induced by vehicle exhaust: A crude oil refinery and ship emissions. *Atmos. Res.* **2013**, *120–121*, 43–54. [[CrossRef](#)]
49. Baldasano, J.M.; Soret, A.; Guevara, M.; Martínez, F.; Gassó, S. Integrated assessment of air pollution using observations and modelling in Santa Cruz de Tenerife (Canary Islands). *Sci. Total Environ.* **2014**, *473–474*, 576–588. [[CrossRef](#)] [[PubMed](#)]
50. Rodríguez, S.; Alastuey, A.; Alonso-Pérez, S.; Querol, X.; Cuevas, E.; Abreu-Afonso, J.; Viana, M.; Pérez, N.; Pandolfi, M.; De La Rosa, J. Transport of desert dust mixed with North African industrial pollutants in the subtropical Saharan Air Layer. *Atmos. Chem. Phys.* **2011**, *11*, 6663–6685. [[CrossRef](#)]
51. Escudero, M.; Castillo, S.; Querol, X.; Avila, A.; Alarcón, M.; Viana, M.M.; Alastuey, A.; Cuevas, E.; Rodríguez, S. Wet and dry African dust episodes over eastern Spain. *J. Geophys. Res. D Atmos.* **2005**, *110*, 1–15. [[CrossRef](#)]
52. Finayson-Pitts, B.; Pitts, J. *Chemistry of the Upper and Lower Atmosphere*; Academic Press: San Diego, CA, USA, 1999.
53. Krueger, B.J.; Grassian, V.H.; Cowin, J.P.; Laskin, A. Heterogeneous chemistry of individual mineral dust particles from different dust source regions: The importance of particle mineralogy. *Atmos. Environ.* **2004**, *38*, 6253–6261. [[CrossRef](#)]
54. Löye-Pilot, M.D.; Martin, J.M.; Morelli, J. Influence of Saharan dust on the rain acidity and atmospheric input to the Mediterranean. *Nature* **1986**, *321*, 427–428. [[CrossRef](#)]
55. Avila, A.; Alarcón, M.; Castillo, S.; Escudero, M.; Orellana, J.G.; Masqué, P.; Querol, X. Variation of soluble and insoluble calcium in red rains related to dust sources and transport patterns from North Africa to northeastern Spain. *J. Geophys. Res. Atmos.* **2007**, *112*, 1–14. [[CrossRef](#)]
56. Querol, X.; Alastuey, A.; Moreno, T.; Viana, M.M.; Castillo, S.; Pey, J.; Rodríguez, S.; Artiñano, B.; Salvador, P.; Sánchez, M.; et al. Spatial and temporal variations in airborne particulate matter (PM₁₀ and PM_{2.5}) across Spain 1999–2005. *Atmos. Environ.* **2008**, *42*, 3964–3979. [[CrossRef](#)]
57. Koçak, M.; Nimmo, M.; Kubilay, N.; Herut, B. Spatio-temporal aerosol trace metal concentrations and sources in the Levantine Basin of the Eastern Mediterranean. *Atmos. Environ.* **2004**, *38*, 2133–2144. [[CrossRef](#)]
58. Mihajlidi-Zelic, A.; Dersek-Timotic, I.; Relic, D.; Popovic, A.; Dordevic, D. Contribution of marine and continental aerosols to the content of major ions in the precipitation of the central Mediterranean. *Sci. Total Environ.* **2006**, *370*, 441–451. [[CrossRef](#)] [[PubMed](#)]
59. Wolaver, T.G.; Lieth, H. Precipitation chemistry. In *Theory and Quantitative Models*; University North Carolina: Chapel Hill, NC, USA, 1972; pp. 15–20.
60. Izquierdo, R.; Alarcón, M.; Aguiillaume, L.; Ávila, A. Effects of teleconnection patterns on the atmospheric routes, precipitation and deposition amounts in the north-eastern Iberian Peninsula. *Atmos. Environ.* **2014**, *89*, 482–490. [[CrossRef](#)]
61. Zhang, D.; Shi, G.Y.; Iwasaka, Y.; Hu, M. Mixture of sulfate and nitrate in coastal atmospheric aerosols: Individual particle studies in Qingdao (36°04' N, 120°21' E), China. *Atmos. Environ.* **2000**, *34*, 2669–2679. [[CrossRef](#)]
62. Fan, S.-M.; Horowitz, L.W.; Levy, H.; Moxim, W.J. Impact of air pollution on wet deposition of mineral dust aerosols. *Geophys. Res. Lett.* **2004**, *31*, 2–5. [[CrossRef](#)]
63. Aguiillaume, L.; Izquierda-Rojano, S.; García-Gómez, H.; Elustondo, D.; Santamaría, J.M.; Alonso, R.; Avila, A. Dry deposition and canopy uptake in Mediterranean holm-oak forests estimated with a canopy budget model: A focus on N estimations. *Atmos. Environ.* **2017**, *152*, 191–200. [[CrossRef](#)]

